Proc. Natl. Acad. Sci. USA
Vol. 87, pp. 8785–8789, November 1990
Biophysics

Sustained vortex-like waves in normal isolated ventricular muscle

(excitable media/heart/rotors/optical mapping/voltage-sensitive dyes)

JORGE M. DAVIDENKO*†, PAUL F. KENT‡, DANTE R. CHIALVO*, DONALD C. MICHAELS*, AND JOSE JALIFE*

Departments of *Pharmacology and ‡Physiology, State University of New York Health Science Center at Syracuse, Syracuse, NY 13210

Communicated by John Ross, July 24, 1990

ABSTRACT **Sustained reentrant excitation may be initiated in small (20 × 20 × <0.6 mm) preparations of normal ventricular muscle. A single appropriately timed premature electrical stimulus applied perpendicularly to the wake of a propagating quasiplanar wavefront gives rise to circulation of self-sustaining excitation waves, which pivot at high frequency (5–7 Hz) around a relatively small "phaseless" region. Such a region develops only very low amplitude depolarizations. Once initiated, most episodes of reentrant activity last indefinitely but can be interrupted by the application of an appropriately timed electrical stimulus. The entire course of the electrical activity is visualized with high temporal and spatial resolution, as well as high signal-to-noise ratio, using voltage-sensitive dyes and optical mapping. Two- and three-dimensional graphics of the fluorescence changes recorded by a 10 × 10 photodiode array from a surface of 12 × 12 mm provide sequential images (every msec) of voltage distribution during a reentrant vortex. The results suggest that two-dimensional vortex-like reentry in cardiac muscle is analogous to spiral waves in other biological and chemical excitable media.**

Many hypotheses have been postulated to explain reentrant excitation in cardiac muscle. Beginning with the classical studies of Mines (1), in which reentry occurs around an anatomical obstacle, through Allessie's leading circle hypothesis (2), to the more recently postulated anisotropic reentry (3), most mechanisms proposed by experimental electrophysiologists are focused on preexisting functional or anatomical inhomogeneities in the myocardium. On the other hand, theoretical studies based on wave propagation in other types of excitable media such as, for example, the Belousov–Zhabotinsky reaction (4) suggest that these rotating waves, also known as "spiral waves," "reverberators," and "vortices," may occur even in totally homogeneous and continuous media (4–8). As proposed by Winfree (9) and later shown in the whole heart (10), initiation of reentry depends not only on the properties inherent to the myocardium but also on transient local conditions created by the impulse that triggers the reentry. In fact, reentrant excitation may be initiated in the myocardium at a critical point that results from the interaction of a geometrically graded recovery of excitation (i.e., the "tail" of a planar wavefront) with a geometrically graded transverse premature stimulus (10). Our objective was to utilize these concepts to develop an *in vitro* model of sustained reentry, in which the electrical activity can be closely monitored. Here we demonstrate that self-sustaining vortex-like reentry can be induced in small two-dimensional pieces of cardiac muscle and that the entire course of the excitation–recovery process during the reentrant cycle can be analyzed in detail through the use of optical mapping and voltage-sensitive dyes.

The publication costs of this article were defrayed in part by page charge payment. This article must therefore be hereby marked "*advertisement*" in accordance with 18 U.S.C. §1734 solely to indicate this fact.

METHODS

Hearts were dissected from anesthetized sheep (sodium pentobarbital, 35 mg/kg, i.v.). Thin slices of left ventricular epicardial muscle (approximately 20 × 20 × 0.5 mm) were dissected by using a dermatome. Suitable preparations were placed in a Plexiglas chamber and superfused with Tyrode solution containing (in mM) NaCl, 130.0; KCl, 4.0; $NaHCO_3$, 24.0; NaH_2PO_4, 1.2; $MgCl_2$, 1.8; and glucose, 5.6. Solutions were saturated with a gas mixture of 95% O_2/5% CO_2. Temperature was maintained at 37 ± 0.5°C and the pH was 7.4. Transmembrane potentials were recorded using glass microelectrodes filled with 3 M KCl and connected to a WPI 750 dual microprobe system. Digitized signals (Neuro-Corder, model DR 484) were displayed on a Tektronix oscilloscope, model 5223. Following control microelectrode recordings, appropriate stimulus parameters were determined for consistent and reproducible induction and termination of self-sustaining high-frequency repetitive activity (see Stimulation Protocol). Subsequently, the preparations were stained for 20 min by superfusion with Tyrode solution containing the voltage-sensitive dye di-4-ANEPPS (4-{2-[6-(dibutylamino)-2-naphthalenyl]ethenyl}-1-(3-sulfopropyl) pyridinium hydroxide; Molecular Probes; 4.5 μg/ml) and then superfused with Tyrode solution containing the electromechanical uncoupler diacetyl monoxime (10 mM). At the end of the experiment, three preparations were histologically analyzed under light microscopy to accurately determine the thickness of the specimen, the fiber orientation, the presence of bands of connective tissue, and the presence of abnormal or damaged tissue. Specimens were fixed in formalin, embedded in paraffin, and stained with hematoxylin/eosin.

Optics and Electronics. We used epi-illumination to project a real fluorescence image of the object stained with di-4-ANEPPS onto a 10 × 10 (minus one) photodiode array (Centronics). The quasimonochromatic light (excitation filter centered at 490 nm; band pass, 90 nm) from a tungsten/halogen lamp was collimated, reflected 90° from a dichroic mirror (560 nm), and focused onto the preparation with an aspheric objective lens. The fluorescence emitted by the preparation was transmitted through the dichroic mirror and an emission filter (centered at 645 nm; band pass, 130 nm) and finally focused onto the photodiode array. By varying the objective lenses, magnifications from 1 to 7 times could be achieved. With a magnification of 4× and with each photodiode being 1.4 × 1.4 mm, each photodiode will receive fluorescence from a square of 1.2 × 1.2 mm of tissue. In this case the total sample area is 12 × 12 mm. The output of each photodiode was connected to a current–voltage converter. The signal was low-pass filtered (time constant: 10.3 sec) and amplified by a factor of 1000. The outputs of the amplifiers were connected to two 64-channel analog/digital boards (12 bit) to achieve 99 channels. The 99 channels were sequentially digitized (12 bits) in 900 μsec. This allowed all of the 99

†To whom reprint requests should be addressed at: Department of Pharmacology, SUNY Health Science Center at Syracuse, 766 Irving Avenue, Syracuse, NY 13210.

channels to be sampled once every msec. The digitized data were then transferred to memory with a 22-bit direct memory access board. After processing, the signals were visualized on a Tektronix storage oscilloscope with the *x-y* display driven by the output of a D/A converter (12 bit). Files were transferred to an IBM AT computer or to a SUN 4/110 work station for further processing and graphics display.

Stimulation Protocol. Four pairs of long (20 mm) Ag/AgCl electrodes were embedded in the wax floor of the chamber in a square array (see Fig. 2*a*). Basic stimulation (S_1) was applied through one of the pairs with trains of 10 pulses (20-msec duration and two times threshold intensity). Single premature stimuli (S_2) 2–20 msec in duration were delivered following every 10th basic response. The intensity and coupling interval of the premature stimulus were varied in a stepwise manner. Premature stimulation was applied to create a voltage gradient perpendicular to the direction of the wavefront (6). To generate such a gradient, the positive and negative poles of the stimulating source were connected to electrodes in contact with opposite sides of the preparation. For instance, if S_1 was applied through electrode pair A, then S_2 stimulation was applied through one pole of electrode B and one pole of electrode D (see Fig. 2). This combination could be easily modified during the experiment. S_2 stimulation was also applied at varying intervals during the reentrant activity to terminate the arrhythmia.

RESULTS

The combination of di-4-ANEPPS and diacetyl monoxime allowed us to obtain signals with high (>30:1) signal-to-noise ratio and totally devoid of mechanical artifact. Fig. 1 shows the 99 optical signals obtained from a thinly sliced piece (21 × 17 × 0.6 mm; note that histological analysis of three preparations showed that they were never thicker than 0.6 mm) of sheep epicardial muscle during propagation of a quasiplanar wave initiated by an extracellular stimulus applied to the top border of the tissue (asterisks). Activation and repolarization patterns could be accurately determined by analyzing the upstrokes (Fig. 1*b*) and the downstrokes (Fig. 1*c*), respectively, of the action potentials. Three-dimensional plots of fluorescence versus position in the *x* and *y* directions were obtained at various times during the course of the propagation process. The top frames of Fig. 1*d* show the activation front advancing from top to bottom and from right to left. Conduction is faster over the left margin, in a direction parallel to the longitudinal axis (arrow labeled L) of the fibers. Although the repolarizing process (bottom frames of Fig. 1*d*) follows the general sequence of activation, it is not totally uniform. Such nonuniformity was always demonstrable, in spite of the fact that all preparations studied were relatively homogeneous in terms of gross morphology and fiber orientation. In fact, histological studies of three preparations failed to find abnormalities or gross irregularities.

Sustained reentrant activity was consistently generated in small pieces of sheep epicardial muscle in all seven preparations. The rotation period varied from 5 to 7 Hz. The results obtained in one experiment are summarized in Figs. 2–4. S_1 stimulation was delivered to electrode B and premature stimulation was delivered through electrodes A (+) and C (−) (see Fig. 2*a*). The arrhythmia was reproducibly initiated by S_2 with the following stimulus parameters: duration, 20 msec; intensity, 4–6 V; and coupling interval, 130–140 msec. Similar S_2 parameters were necessary to terminate the self-sustaining repetitive activity. Fig. 2*b* shows the intracellular microelectrode recordings obtained during initiation and termination of the arrhythmia. Note that the digitized signals obtained with intracellular microelectrodes are comparable to those obtained with the optical system (Fig. 2*c*) from the same region of the preparation (asterisk) during basic stimulation and sustained excitation.

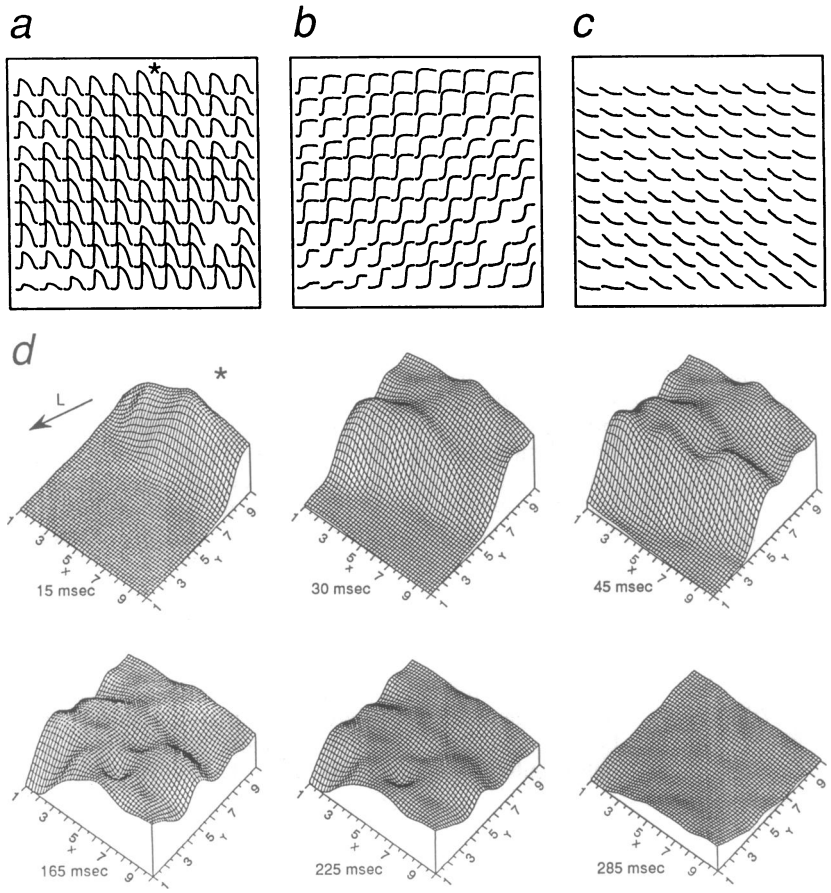

FIG. 1. High resolution of optical mapping. (*a*) Trace duration, 400 msec. (*b* and *c*) Upstroke and downstroke (end of repolarization phase) at a rapid sweep speed (trace duration, 100 msec). (*d*) Three-dimensional representation of fluorescence changes obtained at various times during the course of the propagation process. The relative amplitude of the fluorescence change (*z* axis) obtained from each photodiode was assigned to a point (not to a surface) in the *x–y* grid. To improve visualization of the phenomenon, four additional points were interpolated between the actual data points.

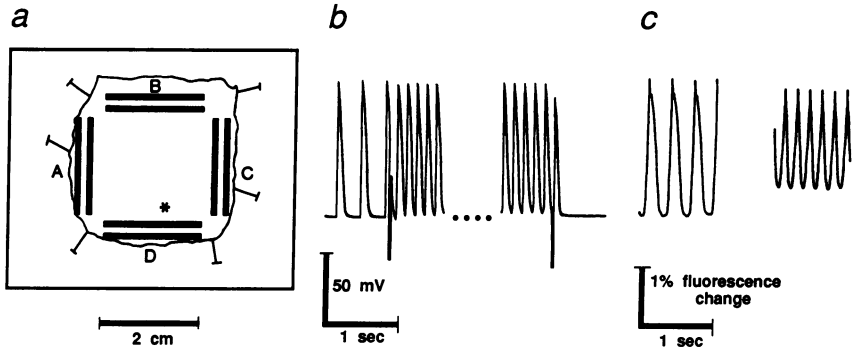

FIG. 2. (*a*) Schematic of the preparation and the stimulating electrodes (black bars). Preparations were driven by trains of 10 basic stimuli (S_1) applied through electrode pair B. The asterisk indicates the approximate region of intracellular and optical recordings. (*b*) Intracellular microelectrode recording obtained during the initiation and termination of the arrhythmia by a single stimulus. Digitizing of the signals introduced some distortion. The ellipsis indicates 3 sec deleted from the continuous record. (*c*) Single optical recording obtained during basic stimulation (left) and during a new episode of reentry (right).

The complete activation–recovery process generated by the sustained reentrant arrhythmia during one full cycle is readily visualized in the three-dimensional color plots presented in Fig. 3. The excitation wave rotates for an indefinite number of cycles in a clockwise manner around a central area with no activity, surrounded by a region of low voltage activity. The diameter of this area, so-called core of the vortex, is 3–5 mm. Some action potentials within this region show double component upstrokes (see below). The main axis of this central region is parallel to the fiber orientation and the speed of propagation of the wavefront is not uniform (approximately 0.2 mm/msec over the anterior and posterior borders and 0.4 mm/msec over the lateral borders) owing to the anisotropy of the tissue. Moreover, within a given frame, the excitation process occupies only one-fourth to one-half of the tissue. Thus, if one considers that the refractory period of each element lasts approximately the same as the total action potential duration, then a topographical distribution of the "excitable gap" (i.e., the time interval during which part of the circuit is excitable) can be precisely determined. In this preparation, the excitable gap varies from 85 to 127 msec, which represents at least half of the rotation period.

Annihilation of the circulation was the result of the collision of the rotating wave with an additional excitation wave generated by a properly timed stimulus. In Fig. 4, the external pulse, delivered to the left border of the preparation (vertical bar), activated only the region that had already recovered (excitable gap) from the previous reentrant activation. This new wavefront advanced in a direction (counterclockwise) that was opposite to that of the rotating process and collided with it a few msec later. This collision produced complete suppression of the activity.

Uniform and nonuniform anisotropy may certainly play a role in the initiation, location, and size of the vortices as well as in the revolution time and direction of rotation (2). However, all of these features may be much more dependent on the characteristics of the initiating stimulation: timing, intensity, and configuration of the stimulating electrodes (9, 10) with anisotropy playing a modulating role. In fact, we were able to modify the rotation of the vortex and the location of the central region, by changing such stimulus parameters. Fig. 5 shows two different episodes of reentrant excitation generated sequentially in another preparation. In both cases basic stimulation (S_1) applied from electrode C generated a leftward moving quasiplanar wavefront, which was parallel to the main axis of the fibers (not shown). A premature pulse (S_2), applied to the bottom of the preparation, resulted in the formation of a vortex with counterclockwise rotation (Fig. 5*a*). After interrupting this circulation, it was possible to initiate a different rotor with clockwise rotation by now applying S_2 to the top portion of the tissue (Fig. 5*b*). Although conduction velocity was nonuniform in either case, the spatial distribution of conduction velocities was different in both. The total revolution time increased from 170 msec in Fig. 5*a* to 205 msec in Fig. 5*b*.

Fig. 5*c* shows the fluorescence changes recorded by the 99 photodiodes during counterclockwise rotation (left; rotation time, 170 msec), basic stimulation (center; basic cycle length, 220 msec), and clockwise rotation (right; rotation time, 205 msec). Action potentials observed during basic stimulation were not uniform. A region of lower action potential amplitude is present in the central region of the recording area. Moreover, nonuniformity markedly increased during the episodes of reentry, which evidenced very low amplitude

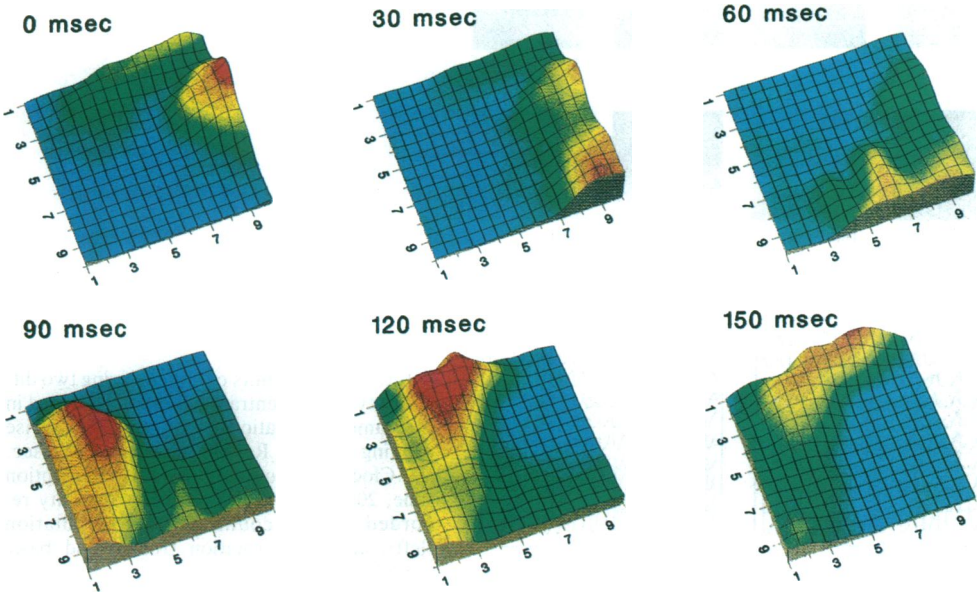

FIG. 3. Three-dimensional color maps of fluorescence obtained from an area of 12 × 12 mm, at six equally spaced intervals, during an episode of sustained reentry. Numbers on top of each frame indicate the time from the first frame. The color spectrum indicates relative fluorescence detected by the photodiode array, with red correlating with peak depolarization and blue correlating with resting membrane potential. The excitation wave proceeds in a clockwise rotation, with a revolution time of 160 msec. Local differences in conduction velocity and action potential duration may account for the presence of several hills and valleys following the head of the activation front.

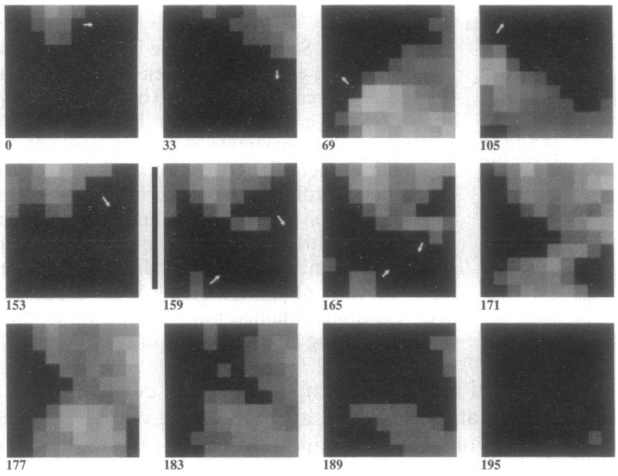

FIG. 4. Annihilation of reentrant activity. Two-dimensional maps of fluorescence changes recorded from the same experiment shown in Figs. 2 and 3. To improve visualization, only regions showing 30–100% maximum fluorescence are differentiated from the background. The upper row of frames shows a complete reentrant cycle (see arrows). The middle row shows the continuous rotation of the wave and also the onset of a second excitation wave induced by external stimulation (vertical bar). Collision of both wavefronts is followed by suppression of the activity.

(subthreshold) responses and two-component upstrokes in the area corresponding to the center of the rotor. In addition, the area of subthreshold responses changed in size and location from one episode of reentry to the other. The diameter of the core was approximately 4 mm during counterclockwise rotation and 2.5 mm during clockwise rotation. This suggests that the region of subthreshold activity during the reentrant process was functionally determined.

DISCUSSION

In the last 10 years, *in vivo* and *in vitro* models of two-dimensional reentry, in which the electrical activity is mapped with good spatial resolution by means of multiple extracellular electrodes, have provided relatively accurate information about the excitation wavefront (11, 12). On the other hand, intracellular microelectrode techniques have provided information on the entire excitation process but with poor spatial resolution, or, alternatively, in a sequential manner (13–15). The ultimate analysis of the mechanisms underlying reentry requires high temporal and spatial resolution as well as the ability to obtain data from all different phases of the local activation process (i.e., transmembrane electrical activity). The use of voltage-sensitive dyes and optical mapping with a photodiode array provides such a resolution and gives direct access to the analysis of the electrical events occurring in the tissue throughout the entire cycle.

One of the major technical difficulties for optical recording from the heart is the mechanical artifact produced by the contraction. Except for the upstroke, the electrical signal during the activation cycle may be severely distorted by such an artifact. Investigators have attempted to overcome this limitation, by sandwiching the heart between two glass windows and pressing Lucite pads against the two other sides of the heart (16). In other cases, the preparations were superfused with calcium-free solutions (17, 18). In our experiments, we have elected to superfuse the preparations with Tyrode solution containing diacetyl monoxime, which is known to totally suppress contractility without altering the electrical activity (19). We also utilized a highly sensitive dye, di-4-ANEPPS (20), which markedly increased the signal-to-noise ratio. Moreover, there has been recent evidence demonstrating good correlation between the signal obtained with a voltage-sensitive dye and that recorded with intracellular electrodes (21). In the case of our mapping set-up, each photodiode receives light from an area of 0.14–1.44 mm^2, so that the signal generated represents the activity of approximately 20–150 cells. Some distortion of the "action potential" morphology is expected under these conditions. Nevertheless, we have compared the duration of the optical signals obtained with a typical magnification of 4× (corresponding to an area of about 0.1 mm^2 monitored by a single photodiode) during normal propagation with those recorded from the same region of the preparation with intracellular microelectrodes. The "optical action potential" was 10–25% longer than the action potential obtained with microelectrodes, which is not surprising since the optical event represents the ensemble average of the activity of as many as 150 cells.

Sustained reentry may be induced in a small piece of rabbit atrium in the absence of anatomical obstacle (2). Unidirec-

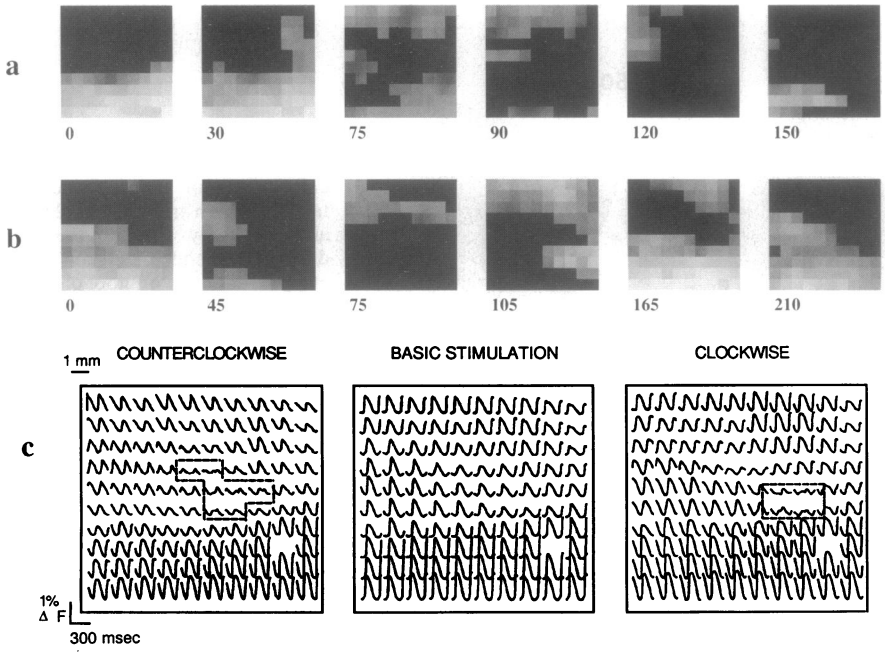

FIG. 5. Snapshots obtained during two different types of reentrant episodes generated in the same preparation. (*a*) Counterclockwise rotating reentry. Revolution time, 170 msec. (*b*) Clockwise rotating reentry. Revolution time, 205 msec. (*c*) Fluorescence activity recorded during counterclockwise rotation (left), clockwise rotation (right), and basic stimulation (center).

tional block, which leads to initiation of such repetitive activity, so-called "leading circle," is usually attributed to intrinsic nonuniformity in the recovery of excitability. Accordingly, a premature wavefront would be blocked in an area of relatively prolonged refractoriness but could propagate through an alternative pathway in which recovery occurs more promptly, thus setting the stage for reentry. It has been recently proposed (7, 9) that leading-circle reentry may in fact be the result of the formation of a rotor giving rise to spiral waves. Such waves would be analogous to those occurring in other excitable media, which are totally homogeneous (4–8). Winfree's theory suggests that rotors may be initiated in an idealized homogeneous two-dimensional piece of cardiac muscle by the application of a premature electrical stimulus some specified time after the tissue has been excited by a propagating planar wave. In a homogeneous system, the tail of the excitation wave represents a uniformly graded dispersion of refractoriness. Hence, the conditions established at the point of intersection (i.e., the "critical" point) of the voltage gradient created by a premature stimulus of critical timing and magnitude with the graded recovery of excitability at the wake of the planar wave should allow the formation of a rotor (9). The direction of the rotor would be either clockwise or counterclockwise, depending upon the specific direction of basic and premature wavefronts. This critical point concept has been supported recently by multiple electrode mapping experiments in the open-chest dog (10). Those experiments established that the critical voltage gradient for the induction of reentry is about 5 V/cm, which is within the range predicted by Winfree. The direction of the rotation was also modified by changing the position of the stimulating electrodes. Our experiments demonstrate that similar concepts apply to two-dimensional pieces of ventricular epicardial muscle. Although we have not as yet measured the critical voltage gradient for our preparations, sustained reentry was induced by the application of a premature voltage gradient that was perpendicular to the direction of a propagating quasiplanar wavefront. In every case, self-sustaining reentry was shown to last for many cycles and was interrupted only if an appropriate stimulus was applied.

A clear advantage of the present model is that it allows the possibility of recording simultaneously the membrane voltage changes occurring at 99 closely apposed sites throughout the entire cycle of rotation. Vortex core diameter has been reported to be about 11 mm on healthy dog ventricles (10) and about 10–20 mm in healthy rabbit ventricle (2). In our experiments, the core diameter varied from 1.8 to 5 mm. Although the discrepancy may be attributed to interspecies differences, it may also be the result of the differences in the recording techniques. Establishing the area of block (i.e., core) with extracellular electrical recordings requires the assumption of an arbitrary value of minimum conduction velocity (10). Optical mapping, on the other hand, allowed the direct measurement of the size of the core on the basis of morphological changes in the action potentials recorded through the voltage-sensitive dye. Assumption of a minimum conduction velocity is not necessary using this technique. Moreover, information on the regional distribution of action potential morphology during paced and reentrant activity, as well as on the duration of the excitable gap and its interaction with the electrical stimulus that terminates the arrhythmia, is readily available for analysis with this technique. Previously, the excitable gap of reentrant processes occurring in the absence of anatomical obstacles was thought to be very small or absent (2). Our results also show that the excitable gap may be relatively long and nonuniformly distributed throughout the preparation. In addition, our results indicate that although altered propagation characteristics occur in a relatively large central region of the preparation, only a small area remains totally inactive during the entire rotation process. Isochrone maps obtained with classical extracellular recordings may, in these cases, show long lines of block. On the other hand, the optical recordings are in agreement with the concept that functionally determined reentry may occur around a small pivot region (i.e., phaseless region).

CONCLUSIONS

Self-sustaining two-dimensional rotating waves may be initiated by single premature electrical stimulation in relatively small pieces of normal epicardial muscle. Such waves may be visualized directly with the optical mapping and voltage-sensitive dyes. Indeed, results obtained in multiple electrode mapping experiments *in vivo* (6) were reproduced in *in vitro* experiments utilizing similar stimulation protocols, with the advantage that the entire activation–recovery process could be determined with substantial accuracy and resolution. During self-sustaining reentrant activity, the center of the vortex is comprised of a relatively small group of cells that show only minimal depolarizations (phaseless region) throughout the cycle. Moreover, the termination of the vortex depends on the interaction of an appropriately timed excitation with the reentrant wavefront moving into the excitable gap. Finally, although uniform and nonuniform anisotropy may account for some of the characteristics of reentry in normal myocardium, the interplay between specific characteristics of the initiating stimulus and the recovery from a previous excitation may play a more important role in establishing the vortex, the phaseless region, and the direction of rotation. Thus, circulation of waves in ventricular myocardium may indeed be the result of generic aspects of excitability rather than of the particular characteristics of the medium (9).

We thank Edward Matyas and Catherine Devine (Cornell National Supercomputer Facility) for their help in the graphic display of the results, Margaret LaVerne Gilbert for typing the manuscript, Dr. Jerry Gordon for the histological studies, and Dr. Maxwell Mozell for the use of his laboratory and equipment. We especially thank Drs. Arthur T. Winfree and Leon Glass for reading the manuscript. This work was supported by grants from the National Institutes of Health and the National Science Foundation.

1. Mines, G. R. (1913) *J. Physiol. (London)* **46,** 349–383.
2. Allessie, M. A., Bonke, F. M. & Schopman, F. J. G. (1977) *Circ. Res.* **41,** 9–18.
3. Dillon, S. M., Allessie, M. A., Ursell, P. C. & Wit, A. L. (1988) *Circ. Res.* **63,** 182–206.
4. Winfree, A. T. (1987) *When Time Breaks Down: The Three-Dimensional Dynamics of Electromechanical Waves and Cardiac Arrhythmias* (Princeton Univ. Press, Princeton, NJ), pp. 154–186.
5. Winfree, A. T. & Strogatz, S. H. (1984) *Nature (London)* **311,** 611–615.
6. Zykov, V. S. (1987) *Simulation of Wave Process in Excitable Media* (Biddles, Guilford, U.K.), pp. 1–43.
7. Krinsky, V. I. (1984) in *Self-Organization: Autowaves and Structures Far from Equilibrium*, ed. Krinsky, V. I. (Springer, Berlin), pp. 9–18.
8. Keener, J. P. (1986) *SIAM J. Appl. Math.* **46,** 1039–1056.
9. Winfree, A. T. (1989) *J. Theor. Biol.* **138,** 271–412.
10. Frazier, D. W., Wolf, P. D., Wharton, J. M., Tang, A. S. L., Smith, W. M. & Ideker, R. E. (1989) *J. Clin. Invest.* **83,** 1039–1052.
11. Janse, M. J. & Wit, A. L. (1989) *Physiol. Rev.* **69,** 1049–1169.
12. El-Sherif, N., Smith, R. A. & Evans, K. (1981) *Circ. Res.* **49,** 255–265.
13. Wit, A. L., Hoffman, B. F. & Cranefield, P. F. (1972) *Circ. Res.* **30,** 1–10.
14. Allessie, M. A., Bonke, F. I. M. & Schopman, F. J. G. (1976) *Circ. Res.* **39,** 168–177.
15. Kamiyama, A., Eguchi, K. & Shibayama, R. (1986) *Jpn. Circ. J.* **50,** 56–73.
16. Salama, G., Lombardi, R. & Elson, J. (1987) *Am. J. Physiol.* **252,** H384–H394.
17. Hill, B. C. & Courtney, K. R. (1987) *Am. Biomed. Eng.* **15,** 567–577.
18. Sawanobori, T., Hirano, Y., Hirota, A. & Fujii, S. (1984) *Am. J. Physiol.* **247,** H185–H194.
19. Li, T., Sperelakis, N., Teneick, R. E. & Solaro, R. J. (1985) *J. Pharmacol. Exp. Ther.* **232,** 688–695.
20. Muller, W., Windish, H. & Tritthart, H. A. (1989) *Biophys. J.* **56,** 623–629.
21. Gupta, R. K., Salzberg, B. M., Grinvald, A., Cohen, L. B., Kamino, K., Lesher, S., Boyle, M. B., Waggoner, A. S. & Wang, C. H. (1981) *J. Membr. Biol.* **58,** 123–137.